



Biological Application of Zinc Oxide Nanoparticles Created by Green Method



Mohamed A. Abdelhady^{1*}, Tarek M. Abdelghany², Sonya H. Mohamed¹ and Salah A. Abdelhamed²

CrossMark

¹ Department of Agricultural Microbiology, Soil, Water and Environmental Research Institute, Agricultural Research Center, 12619, Giza, Egypt

² Botany and Microbiology Department, Faculty of Science, Al-Azhar University, Cairo 11725, Egypt

IN THE WORLD, *Ralstonia solanacearum*, the second most harmful bacterial phytopathogen, poses a serious danger to potato crop by causing brown rot disease, which can result in losses of up to 100%. For that, this study aims to isolate and identify of pathogenic bacteria causing brown rot disease and biocontrol it using ZnONPs synthesized by fungal strain. Eighteen infected potato cv. Cara samples were collected from different six regions of El-Minya governorate, Egypt. Isolation, identification and pathogenicity test were done for the most common pathogenic bacteria. Also, 18 native agricultural soil samples from 6 regions of El-Minya governorate, Egypt. Additionally, isolation and identification for the most common fungal isolate able to synthesize ZnONPs. Mycosynthesized ZnONPs was characterized by UV, TEM, SEM, EDX, XRD, FTIR, Zeta potential and particle size. Cytotoxicity test for mycosynthesized ZnONPs was done to determine safety level of obtained nanoparticles which its dominant spherical or hexagonal shapes and small in size at 42.2 ± 3.0 nm. Results showed that the pathogenic bacterial isolate was identified using morphological, biochemical and molecular as *Ralstonia solanacearum* (OR533702). Also, 16 fungal isolates were isolated and the most common was selected and identified as *Epicoccum nigrum* (OR533699) using microscopic, macroscopic and molecular identification. Additionally result showed the selected fungal strain *E. nigrum* has high efficacy with inhibition zone diameter (2.20 ± 0.20) mm at 100 $\mu\text{g}/\text{mL}$ (5mM) against *R. solanacearum*. This study concluded that mycosynthesized ZnONPs has potent effect against *R. solanacearum* compared to Revanol 50% as traditional product.

Key words: Biological control, *Ralstonia solanacearum*, Potato tubers, ZnONPs, Biosynthesized.

1. Introduction

Twenty tow percentage of the Potato crop was lost due to biological pests and pathogenic microorganisms, led to significant economic damage (Alyokhin et al., 2022; Masmoudi et al., 2023). Increased exposure to diseases including Brown rot, Potato viruses, Early blight, Black leg, Late blight, Wilt, Scab and Black scurf among others, which are present in soil, potato tubers and the airborne which Each year, plants exposure tremendous losses due to soil-borne plant diseases. *R. solanacearum* is the 2nd most harmful phytopathogen bacterium over the world among them related to its destructive tendency. This dangerous disease infects about 310 plant species belong 42 family of plants. Yield losses due to the pathogen of bacterial wilt reached 20% to 100% globally (Khoshru et al., 2023; Wang et al., 2023).

Potato wilt and tobacco diseases caused by the *R. solanacearum* bacteria species complex pose a

is reducing the yields significantly over the world. The most destructive plant bacterium in the world, Brown rot, which is caused by *Ralstonia solanacearum*, which affects over 50 families of plants, causes significant yield and quality losses reach (5 to 70%), especially in warm growing environments, is one of these diseases (Asaturova et al., 2021; Bastas, 2023).

serious danger to Solanaceae and have an impact on global productivity. The bacterial wilt pathogen caused by *R. solanacearum* infected plants at the roots, the plant vascular system colonized and the xylem tissues blocked. As a result, many solanaceous crops suffer yield losses that can range from 15 to 55 percent worldwide and up to 70 percent after *Phytophthora infestans* which is causing the disease of late blight (Ahmed et al., 2022; Aslam & Mukhtar, 2023). In more than 80 different countries afflicted by *R. solanacearum*,

*Corresponding author e-mail: dr.mohamed334455@gmail.com

Received: 27/02/2024; Accepted: 19/03/2024

DOI: 10.21608/EJSS.2024.272650.1731

©2024 National Information and Documentation Center (NIDOC)

each year's loss of potato fields valued at 1.7 MH amounted to a \$950 million loss (Khairy et al., 2021; Mazurkiewicz-Pisarek et al., 2023). The majority of the potato harvests in this diversity, the cv. Cara variety, have been reported to be susceptible to the brown rot disease (Hassan et al., 2022; Prusky & Romanazzi, 2023).

Ralstonia often moves quickly to the stem tissues after colonizing the tissues of root xylem and invading the roots of resistance plants and susceptible through of minor wounded pores. The intricate xylem, which transports water, is made up of either (parenchyma) as living and (tracheids) as dead cell types, Exopolysaccharides components, which *R. solanacearum* frequently produces, causes obstruction in the xylem, followed by causing in the presence or appearance of wilting in plants (Yadeta & Thomma, 2013; Carter et al., 2023). *R. solanacearum* is ranking the second bacterial plant pathogen around globally, has been found to be a source of soil-borne bacterial infections. It is the cause of the bacterial wilt disease. When plants wilt, bacteria migrate from the plant roots to the soil. *Ralstonia* activates a variety of virulence factors to cause disease in different infection phases (Dey & Sen, 2023; Rivera-Zuluaga et al., 2023).

Nowadays, Nanobiotechnology enables the production of advance intelligent components from synthesized biological structures. Due to their features and distinctive materials, nanoparticles (NPs) have newly gained trust in a variety the scientific fields, including the agricultural industry, the energy sector, environmental sciences and the medical field (Zhao et al., 2020; Chugh et al., 2021; Dina et al., 2022; Mohammad et al., 2023). Myconanotechnology have the ability to produce of nanomaterials at low temperature < 100 °C comparison with > 300 °C needed for chemical synthesis (Shaheen et al., 2021; Srivastava et al., 2022), the protein secretion increase with variations in temperatures, also, the producing of particles rate are improving (Noman et al., 2023).

Most of studies showed that fungi have the ability in bioproduction and biosynthesis of nanoparticles in the large scale because large amounts production of extracellular enzymes, from this species *Fusarium oxysporum*, *Aspergillus flavus* and all of them play role in intracellular and extracellular nanoparticles synthesis, also, the fungi have shown great potential for the production of nanoparticles which contain the downstream processing, biology system, synthetic biology, metabolic engineering and protein engineering (Pantidos & Horsfall, 2014; Meena et al., 2021). Among multi fungi species *Aspergillus* is a very potentiality used in the ZnONPs producing which is more than 350 species from *Aspergillus*, in addition to the protein quantity large secretion, Also, such as, *A. terreus*, *A. fumigatus* and *Trichoderma viride* etc. (Abdelkader et al., 2022; Hashem et al., 2023).

Endophytic fungi have superior against the other endophytic microorganisms which have the native nature; also, more secretion from secondary metabolites that distinguished it than the other microorganisms, this metabolites are essential for native fungus and searching for the antibacterial properties (Ababutain et al., 2021; Oladipo et al., 2022). The ZnONPs used in more of applications, such as catalysis, medical diagnosis, catalysis and various activities like thrombolytic potential, antidiabetic and anticoagulant, in addition, ZnONPs have a role in agriculture sector which used as antibacterial agents (Nasrollahzadeh et al., 2019; Shrestha et al., 2020). The performance of ZnONPs synthetic by *Epicoccum nigrum* indicated that the affectivity against plant pathogens and pests control, also, *E. nigrum* have a biomass materials secretion imported in the plants defense, additionally, the ZnONPs synthesis by *E. nigrum* evaluated as essential role in biological process and biocotrol agents against the others microorganisms especially *Ralstonia solanacearum* causing brown rot disease followed the bacterial pathogens and *Fusarium oxysporum* conducted the fungal pathogens (Yadav et al., 2023).

This study aims to survey, isolation and identification of the pathogenic bacteria causing brown rot disease. Also, isolation and identification of fungal strain synthesized ZnONPs has potent effect against bacterial pathogen causing brown rot disease compared with Revanol 50% as traditional product. Finally, Full characterization of the most potent mycosynthesized ZnONPs is done using UV, TEM, SEM, EDX, XRD, FTIR, Zeta potential and particle size.

2. Materials and Methods

2.1. Media used

Muller Hinton Agar medium (MH) (Åhman et al., 2022), Potato Dextrose Agar (PDA) (Chokboribal et al., 2023), Potato Dextrose broth (PDb) (Tejashwini et al., 2023).

2.2. Chemicals used

Agar was purchased from El-safa (El-minya Gov.), Egypt. Glucose powder and ethanol 70% were purchased from Sugar factory (Abu-qerkas, Egypt). Water filtered and distilled using a Milli-Q system Millipore (Milan, Italy). Sodium hypochlorite solution (1%) was purchased from Otsuka (10th of Ramdan city, Egypt), 20% (v/v) Clorox (Adco, Alex. Egypt), Revanol 50% (Hydroxy-geutoulin-sulfate from Shoura Company, Egypt) used as traditional product, Zinc Oxide nanoparticles (Nano. materials Lab., ARC, Giza, Cairo) as chemical component.

Samples collection

(A) Bacterial pathogen was evaluated and conducted at 18 samples for 6 regions of El-Minya (25°46'29"N 14°55'36"E), Samalout (23°37'18"N 12°52'22"E), Matay (22°38'21"N 13°45'33"E), Beni-mazar (20°32'21"N 11°22'18"E), Maghagha (21°44'25"N 10°46'35"E) & El-Edwa (27°41'23"N 17°50'32"E) of the market in El-Minya governorate where potato is the major crop. In each market cv. Cara potato tubers were examined. Eighteen samples (60-70 tubers/sample/region) from this variety were collected randomly and visually examined for brown rot disease as similar by (Abo-Elnaga et al., 2013). The potato tubers that displayed the same disease symptoms were removed, packed in paper bags, and put in a cooling box that was kept at 7 °C and 85 to 90% relative humidity for further examination.

(B) Native agricultural soil fungal isolates were collected at 18 soil samples for different 6 crops of Mallawy center, El-Minya governorate, Egypt, selected the more common fungal isolate, the samples reserved as the previous in bacterial pathogen isolate. Then transferred the samples to Agri. Micro. Res. Lab., Mallawy of Agri. Res. Stat., ARC. Giza, Egypt, for isolation, identification and pathogenicity procedures of the bacterial pathogen using the method described by (Shen et al., 2022).

2.3. Isolation and identification of bacterial pathogen

The samples of the infected potato tubers characterized with similar symptoms to brown rot disease were selected as a source of bacterial phytopathogenic. Also, isolated bacteria from the potato tubers that infected were as described above, Cores with main vascular and cortical tissues, measuring 5-10 mm in diameter and 5 mm in length, were obtained and macerated in 10 ml of sterilized distilled water for 5 minutes, taken 1 ml from macerated solution, serial-diluted, streaked on Mueller Hinton agar medium with antifungal (Flucoral) and streaked the media on the plates, then examined after incubation period for 24–48 h at 30 °C (Khairy et al., 2021).

2.3.1. Morphological

The morphological identification processes were established by observing the isolated bacteria on MH medium after incubated at 30°C for 24-48h, culture stained by Ziehl-Neelsen as recommended in the 'Manual of microbiological methods, 1957'. The slides were examined under microscope for determination of gram stain, motility, shape and arrangement of cells in faculty of science, Al-Azhar University according to (Pawaskar et al., 2014; Zhang et al., 2022).

2.3.2. Biochemical

The isolated bacteria had been grown in sterilized MH agar medium and incubated for 24-48h at 30°C, sent the isolate to identify at 57357 hospitals in special laboratories used MALDI-TOF MS (Vitek compact 2 apparatus) according to manufacture (Faron et al., 2017).

2.3.3. Molecular

The bacterial isolate was prepared as the previous steps (Altschul et al., 1990). The Molecular Biology Research Unit of Assiut University received cultures. After that, a bacterial DNA sample was sent to SolGent Company in Daejeon, South Korea for PCR and 16S rRNA gene sequencing. Two universal primers, 27F (forward) and 1492 R (reverse), were added to the reaction mixture to be used in PCR. Primer 27F (5'- AGA GTT TGA TCC TGG CTC AG -3') and 1492 R (5'- GGT TAC CTT GTT ACG ACTT -3') are composed as follows. Thermal cycling is defined as the following steps: initial denaturation at 94 °C for 2 - 5 min; cycle of denaturation at 95°C for 30 s; annealing at 55 – 60°C for 1 min; elongation at 72 °C for 60 s, and completion at 72 °C for 5 - 10 min. The same primers and ddNTPs were added to the reaction mixture before sequencing the purified PCR results (amplicons) (Innis & Gelfand, 2012). The Basic Local Alignment Search Tool (BLAST) from the National Center of Biotechnology Information (NCBI) website was used to examine the acquired sequences. <http://blast.ncbi.nlm.nih.gov/Blast.cgi>? Blast p is the program, BLAST Search is the page kind, and blast home is the link location. MegAlign (DNA Star) software version 5.05 was used to perform phylogenetic analysis on the sequences. The phylogenetic tree was inspected and printed out to be included in the results after alignment with closely similar sequences acquired from the gene bank (using the cluster-W approach).

2.3.4. Pathogenicity test of bacterial pathogen

Pathogenicity test for isolated bacteria was performed by two methods: (A) Potato tuber slices: the method was done by sterilized the potato tuber at the surface for 3 minutes in 1.5 % (v/v) sodium hypochlorite solution, rinsed by sterilized distilled water 3 times and allowed on filter paper (Whatman N.1) to drying. Tuber slices (10 mm × 5 cm) for thick and diameter of cv. Cara from each (6 tubers); a scratch (wound) in the mediate of tuber slices 5 mm in the deep nearly, 10 mm wide with scalpel after sterilized it, after prepared the suspension of pathogenic bacteria freshly (24 h), inoculated the wound which placed in the tubers by (100 µL) suspended pathogenic bacteria and sterilized distilled water was used to inoculate negative as control, after the inoculation, tuber slices were placed randomized in plastic trays supplemented with sterilized moist cotton to maintain high humidity and incubated for 48 h at 25 ± 2 °C

followed data was then recorded (Marquez-Villavicencio *et al.*, 2011; Shmas *et al.*, 2016). (B) cv. Cara tubers cultivation in the greenhouse: three replicates were used and plants injected with sterile distilled water served as the control. Surfaces of the aforementioned cv. Cara potato tubers were sterilized with 1.5% Naclo for 3 minutes then washed with sterilized distilled water and planted in plastic pots 30 cm in diameter filled with sterile clay (2 tubers / pot). Plants were directly inoculated when they were 15 to 20 cm long by operating a sterilized needle through to a depth of 0.25 ml and injecting 100 μ L of the suspended pathogenic bacteria. Directly inoculated plants were then kept in a greenhouse at a temperature of 25 ± 2 °C and the development of brown rot disease was examined (Asiry *et al.*, 2021).

2.4. Isolation and identification of fungal isolate producing ZnONPs

To isolation process of the fungi producing ZnONPs, prepare the fungal isolate growth on PDA media after incubated at 28°C for 3-5 days, select one fungus from the all isolates in this study and identify the more common isolate (producing ZnONPs) macroscopically, microscopically in the faculty of Science, Al-azhar University, Cairo, according to (Bavarsad & Farrokhi-Nejad, 2018). Also, molecularly identification used by 18S rRNA in the Molecular Biology Research Unit of Assiut University according to (Edslev *et al.*, 2021).

2.5. Screening and mycosynthesis of ZnONPs

The screening process concluded 16 fungal isolates, select the superior most common isolate to producing of ZnONPs. In order to mycosynthesized ZnONPs, 10 ml of the extraction of fungal mycelia and combined with dis. water (100 mL) before being gently incorporated into a zinc solution (100 mL). A suitable molar mass of 99% pure zinc acetate dehydrate (CH_3COO)₂ H₂O (Sigma, Egypt) is needed to prepare the zinc solution. The salt solution of ZnONPs was made by mixing (183.48 gm/mol multiplied by 1000 = 0.183100 = 18.3480.1 = 1.834 gm of zinc salt) with dis. water (100 mL), heated the mixture at 100 °C for 6 hours in a magnetic stirrer set (250 rpm) by using hot plate. Occur change in the reaction mixture to white color. Then the reaction mixture was centrifuged for 15 min at 15,000 rpm, followed by discard the supernatant, the precipitated nanoparticles were washed, and then transferred into a glass plate, and dried at 300 °C (Fig. 1). The formed dry particles were kept at room temperature (25 °C) for further characterization (Kamal *et al.*, 2023).

2.6. Cytotoxicity evaluation of mycosynthesized ZnONPs on HepG2-vero cells by MTT protocol with Morphological assay

The steps were arranged according to (Alley *et al.*, 1988):

After 24 h of incubated at 37°C with 1×10^5 cells / ml (100 μ L / well), a complete monolayer sheet emerge in the 96-well tissue culture plate. The growth medium from the 96 well micro titer plates will remove once a confluent sheet of cells forming, and the cell monolayer has been times washing with media. The maintenance medium, an RPMI medium comprising 2% serum to dilute the test sample twice. Test 0.1 ml of every dilution in different wells, remaining three wells as controls that had just been given maintenance medium. After an incubation period of 37°C, the plate has examine. The physical signs of toxicity, including partial or total loss of the monolayer, shrinkage, rounding or cell granulation, have examine in individual cells. MTT solution (5mg/ml in PBS) make (BIO BASIC CANADA INC.). 20 μ L of the solution of MTT add in each well for 5 minutes, to carefully incorporate the MTT into the media components, shake at 150 rpm. In an incubator, let the MTT digest for 4 hours at (37C, 5% CO₂), the media was discarded. (If required, dry the dish on tissue paper to get rid of the excess). The metabolic product of MTT (Formazan) dissolve once again in 200 μ l DMSO. Shake at 150 rpm for the 5 minutes to thoroughly blend the formazan and solvent. Read optical density at 560 nm, and then subtract background at 620 nm. Cell count and optical density should be closely.

2.7. Characterization of mycosynthesized ZnONPs

2.7.1. UV-Vis spectra analysis

Ain-Shams University at the central laboratory for the science faculty employed UV-Vis spectrophotometry to determine the ZnONPs maximum absorbance. Utilizing a spectrophotometer (Cary E 500) and ultraviolet and visible absorption spectroscopy, the optical features of ZnONPs were estimated (Abdelghany *et al.*, 2023).

2.7.2. Transmission of electron microscopy (TEM) (TEM) (JEM-1230, JEOL, Akishima, Japan) used to characterize the composition of structures and determine the size of ZnONPs. The samples were put on the copper grid with carbon coating and left there for one minute to create a thin layer. Filter paper was used to remove any extra liquid before it was subsequently put in a grid of box (Abbas *et al.*, 2021).

2.7.3. Scanning of electron microscopy (SEM) & EDX

(SEM) investigated and measured the morphological structure of ZnONPs using a TM-1000 from Hitachi, Japan. An aliquot of each sample was placed on a

grid of copper that had carbon coating, and the film was dried by placing the SEM grid under a mercury lamp for five minutes. To confirm the presence of nanoparticles, the instrument was fitted with an energy dispersive X-ray (EDX) spectroscopy (IT100LA) (Abbas et al., 2021; Dina et al., 2022).

2.7.4. X-ray diffraction (XRD)

The nanoparticles were dried and subjected to (XRD) analyses using a Holland XPert PRO diffractometer with a detector voltage of 40 kV and a current of 30 mA utilizing CuK α radiation. With a speed of scanning at 6 $^\circ$ /min, the reported range at 2 θ was 20–80 $^\circ$ with the help of the Debye-Scherrer's formula; the sizes of the particles were estimated (Abdelghany et al., 2023).

2.7.5. Fourier transform infra-red spectroscopy (FTIR)

In the central of laboratory for the science faculty at Assiut University, using the powder of the mycosynthesized ZnONPs by FTIR vector 22, Bruker, Germany, the spectra properties of ZnONPs were observed. At room temperature, the pellets were scanned at resolution (4 cm $^{-1}$) in the spectral band (4000-400 cm $^{-1}$) (Carmichael & Eugster, 2018; Doaa, 2024).

2.7.6. Evaluation of Zetasizer Nano ZN

Before measurement, the sample was estimated by dispersing 1 mg in 1 ml of deionized water, diluting it to 10X, and then sonicating it for 30 minutes. The prepared particles (particle size and size distribution) as measured in terms of average volume diameters and polydispersity index were analyzed using a Dynamic Light Scattering (DLS) particle size analyzer (Zetasizer Nano ZN, Malvern Panalytical Ltd., United Kingdom) at a fixed angle of 173 $^\circ$ at 25 $^\circ$ C. Each sample was examined three times. Zeta potential measurement was performed using the same tools (Li et al., 2019).

2.8. Biological Application

2.8.1. Determination of mycosynthesized ZnONPs potency against *R. solanacearum*

According to (Abbas et al., 2022). Agar well method with apply to evaluation of the mycosynthesized ZnONPs potency against *R. solanacearum*. Using ZnONPs (100 μ g/mL) 5mM in concentration and compared with other treatments including, control (precursor Zn acetate salt), commercial bactericide (Revanol 50%) as traditional product, Revanol 50% with ZnONPs producing by *E. nigrum*, ZnO as purchased chemical NPs., Revanol 50% with ZnO was tested to check its antibacterial potency, every treatment added separately of MHA (Muller Hinton Agar) media, all treatments used in 3 replicates. *R. solanacearum* was inoculated by 100 μ L to every treatment into the middle of media plates under sterilized conditions, this employed concentration of ZnONPs treatments were applied to the bacterial pathogen and the plates without ZnONPs treatments served as the positive control. The media petri dishes

were incubated for 1-2 days at 30 $^\circ$ C, after incubation period show the varieties in inhibition zones diameter of bacterial pathogen.

2.9. Statistical analysis

Data preparation used the mean \pm standard deviation and standard errors (n=3). All statistical analysis was done with SPSS program version 20.0. (Prajapati et al., 2023).

3. Results

3.1. Evaluation of the bacterial disease in potato tubers

During the potato harvest in market of six regions at El-Minya governorate the potato cultivars cv. Cara that had symptoms of bacterial diseases were examined. The data illustrated in (Table 1) showed that from the 6 regions, El-Edwa and Matay regions recorded the lowest tuber infections by 2 samples for bacterial pathogen from the 5 samples. Where the rest regions (including: El-Minya, Beni-mazar and Maghagha) showed the same tuber infections (3 samples) by bacterial diseases from total samples obtained.

3.2. Disease incidence of bacterial pathogen

Results in (Table 2) indicated that the disease incidence of bacterial disease is significantly differences among the 6 regions were tested. The bacterial disease, El-Minya region had the highest significant increase in disease incidence (2.4 \pm 0.12) followed by Samalout region (2.0 \pm 0.22) and the lowest value was recorded in Matay, El-Edwa regions (0.4 \pm 0.25, 0.4 \pm 0.15) respectively.

3.3. Isolation and identification of bacterial pathogen

Firstly, identify the Symptoms of bacterial disease on potato tubers:

3.3.1. Morphological, macroscopic & microscopic examinations

The symptoms showed during the cross section exhibited in (Fig. 2), the developed stages from healthy potato tubers and infected by isolated bacterial caused brown rot disease whereas oozes appeared on the cells of tubers, converted in to brown color (brown rot disease). Macroscopically showed the isolated bacterial colonies growth as white with pink centers color and mucus shape on petri dish (Fig. 3). Also, when used the microscope indicated that the characters of colony appeared as bacilli (stem chains) (Fig. 4).

3.3.2. Biochemical identification by using MALDI-TOF mass spectrometry

Results in (Table 3) showed the analytical substance of ensured bacterial isolate (*R. solanacearum*) with bionumber (0201704410000200).

3.3.3. Molecular identification of bacterial isolate

The molecular identification of the bacterial isolate was based on genetically by 16S rRNA sequencing (Fig. 5).

3.3.4. Pathogenicity test of bacterial isolate

The isolated bacteria with 24-48h in growth (*R. solanacearum*) inoculated of potato slices cv. Cara. After 2-3 days from the inoculation, the bacteria was growth in the center of potato slices of the wound area that changed to brown color, developed & led to soft tissues compared with the control treatment (Fig. 6). Also, the symptoms appeared after 21 days from the inoculated of potato plant stems which will appear as wilt disease (Fig. 7), the causal agent was *R. solanacearum*.

3.4. Isolation and identification of mycosynthesized fungal isolate

3.4.1. Morphological, macroscopic & microscopic examinations

The fungal isolate was identified primitively, based on general morphological characteristics, macroscopic, as well as color, shape, microscopic (Figs. 8, 9).

3.4.2. Molecular identification

All isolated fungi from the native agricultural soil were studied, selected the more common fungal isolate and used it in ZnONPs synthesized. Genetically identified by 18S rRNA sequencing, and a few other ITS sequences of rDNA from the GenBank search results were used in phylogenetic analysis. A comparison between GenBank search results and the neighboring organism from phylogenetic trees, molecular identify done for isolate with good quality ITS sequencing data and 18S rRNA sequencing showed the organism was identified as *Epicoccum nigrum* (Fig. 10).

3.5. Mycosynthesis of ZnONPs by *E. nigrum*

Primitively, when adding the Zn-acetate to the fungal filtrate solution appeared the color change to white with a magnetic stirrer at 100 °C for 6hrs after incubated in dark, that is primitive evidence on the formation of nanoparticle in the test solution. The solution stored at room temperature after being finely powdered and the characterization process were done as the follow steps (Fig. 1).

3.6. Determination of mycosynthesized ZnONPs cytotoxicity

The functional assay (MTT) experiment design indicated that the mycosynthesized ZnONPs sample had an adverse effect on vero cells, and the data in (Table 4) showed that this effect was concentration dependent. When VERO cells were exposed to ZnONPs at various concentrations for 72 hours, the cells of viability were decayed. The cytotoxicity and

cell viability both markedly decline as the concentration rises.

3.7. Characterizations of mycosynthesized ZnONPs by *E. nigrum*

3.7.1. UV Analysis

The mycosynthesized ZnONPs by *E. nigrum* was identified via spectral analysis with a UV-Vis spectrophotometer showed in (Fig. 11), and mainly exhibit 263.50 nm of absorbance peak, which insured the production of ZnONPs were done.

3.7.2. TEM Study

The ZnONPs were shown in TEM micrographs to have cubic, hexagonal, and spherical shape structures in (Fig. 12), which was matching the SEM image. The typical mean size of the ZnONPs produced by *E. nigrum*, according to TEM micrographs, was 49.0 3.0 nm, followed by 53.2 3.1 nm, and 58.4 3.5 nm. TEM pictures of ZnONPs show the size distribution of particles and magnification 5000_, Bar 145 nm (Fig. 12).

3.7.3. SEM Study

The surface morphology of the produced ZnONPs was investigated using the SEM micrograph of the particles. According to the SEM image in (Fig. 13), the nanoparticles were aggregated and agglomerated. Surfactant can be used to dissolve the agglomeration, but doing so will result in the loss of any possible nanoparticle properties.

3.7.4. EDX Analysis

The detection of ZnONPs with EDX analyzer suggests a zinc ion was converted to a zinc element in the reaction mixture. Zinc and oxygen were founded in sample due to composition of elemental analyzing of ZnONPs (45.27% of Z and 41.35% O), which also showed how pure the manufactured ZnONPs were as shown in (Figs. 14, 15).

3.7.5. XRD Study

By using *E. nigrum*, the XRD investigation identified the produced nanoparticles crystallinity. Using the XRD spectrum, the structural properties of the mycosynthesized ZnONPs were identified. The crystals are just normal atom arrays. Using the XRD patterns, the phase identification, purification, and size of crystallinity were validated as shown in (Fig. 16).

3.7.6. FTIR study

The functional of groups included the mycosynthesized ZnONPs were identified using an FTIR analysis. The measurements were made in the 400 cm⁻¹ to 4000 cm⁻¹ spectral region, which

displayed a variety of absorption bands. The phenolic OH group was visible in the IR spectrum of the mycosynthesized ZnONPs, confirming the potential mechanism for the production of ZnONPs, The strong O-H band of the alcohol is shown by the peak at 3443.55 cm⁻¹. The vibrational modes of the N-O strong bond in nitro compounds and the C-H medium band in alkane compounds, respectively, are founded by the absorption peaks at 1634.79 cm⁻¹ and 1409 cm⁻¹, respectively. The C-Br strong halo molecule is followed for the peaks at 670.59 cm⁻¹, shown in (Fig. 17). The obtained result and the standard JCPDS card no. 01-1136 are in good accord.

3.7.7. Zeta potential & particle size

Coagulation, sonification, and the addition of a stabilizer (such as sodium hexametaphosphate hexamethyl) can all affect the particle size distribution. Dispersant is another crucial component. The zeta potential changed during the titration with NaOH, as seen in (Fig. 18). Furthermore, the sample was monitored of particle size, pH = 7.3, zeta potential was +35 mV, and the particle size was 50 nm during the titration process began. Moreover, zeta potential and particle size measurements were used to establish the stability of ZnO suspensions (Fig. 18).

3.8. Biological Application

3.8.1. Antibacterial Activity of mycosynthesized ZnONPs against *R. solanacearum*

The antibacterial assay was carried out in accordance with the protocol used for zinc oxide. Simply, *R. solanacearum*, isolated from the market of six regions at El-Minya governorate, the potato cultivars cv. Cara that had symptoms of bacterial disease (brown rot disease) were appeared and antibacterial method was completed by using the Agar well method with nanoparticle dispersion to some differentiation. After the MHA media solidified, the autoclaved MHA media with ZnONPs to one concentration of NPs (100 µL/1mg at 5mM) was poured into the wells to every dish. The bacterium was inoculated by loop spreading. Time intervals of 1-2 days were used to measure the effectiveness of the ZnONPs treatment by using measurements of the zones diameter of inhibition around every well. The results of each test were carried out in triplicate and expressed in millimeter (mm). The bacterium growth measured in different treatments of the used concentration of ZnONPs (Figs.19, 20). At control treatment (precursor zinc acetate salt), the inhibition of pathogenic bacteria was 0.50 ± 0.25 mm; at the *E. nigrum* (ZnONPs) as biocontrol treatment of the inhibition was 2.20 ± 0.20 mm; at the commercial bactericide (Revanol 50%) as traditional product the inhibition was 1.85 ± 0.10 mm; at the Revanol with ZnONPs the inhibition was 2.00 ± 0.22 mm; at ZnO purchased chemical treatment the inhibition was 1.54 ± 0.10 mm; at the Revanol with ZnO purchased chemical treatment the inhibition was 2.12 ± 0.08 mm as shown in (Fig 19).

Table 1. Evaluation of bacterial diseases on potato cv. Cara produced in 6 regions at El-Minya gov., Egypt.

Isolate	Regions																	
	El-Minya			Samalout			Matay			Beni-mazar			Maghagha			El-Edwa		
	S1	S2	S3	S1	S2	S3	S1	S2	S3	S1	S2	S3	S1	S2	S3	S1	S2	S3
Bacterial isolate	+	-	-	+	+	+	-	+	-	-	+	-	-	-	+	-	+	-
Total isolates	1			3			1			1			1			1		

+, positive - , negative

Table 2. Average mean of disease incidence (DI) of bacterial disease on potato cv. Cara at 6 regions in El-Minya gov., Egypt.

Regions	El-Minya	Samalout	Matay	Beni-mazar	Maghagha	El-Edwa
Disease Incidence (DI)	2.4 ± 0.12	2.0 ± 0.22	0.4 ± 0.25	1.0 ± 0.36	0.8 ± 0.25	0.4 ± 0.15

Data are mean ± standard errors (n=3).

Table 3. Identification of bacterial isolate by VITEK2 system.

Character (Test)	Abbreviation	Result
Gram stain	GS	-ve
Alaphe proarylamidase	APPA	-ve
LPyrrolidonyl-Arylamidase	PyrA	-ve
Beta- galactosidase	BGAL	-ve
Alpha- galactocidase	AGAL	-ve
(Beta- Glucuronidase)	BGURr	-ve
D-Sorbitol	dSOR	+ve
Sucrose	SAC	+ve
DMannose	dMNE	-ve
Phosphatase	PHOS	-ve
D-maltose	dMAL	+ve
L-Prolin Arylamidase	ProA	-ve
L-Lactate Alkalinization	ILATK	-ve
Tyrosine Arylamidase	TyrA	-ve
O/129 resistance	O129R	-ve
Urease	URE	-ve
Alpha-Mannosidase	AMAN	+ve
Arginine Dihydrolase2	ADH2S	-ve
N- Acetyl- D- Glucosamine	NAGA	-ve
Alpha- glucosidase	AGLU	+ve
D-Amygdalin	AMY	-ve
Leucine Arylamidase	LeuA	-ve
Alanine Arylamidase	ALaA	-ve
D-Ribose	dRIB	-ve
Novobiocin Resistance	NOVO	-ve
D- Raffinose	Draf	-ve
Optochin resistance	OPTO	+ve
Phosphatidylinositol Phospholipase C	PIPLC	-ve
Cyclodextrin	CDEX	-ve
Tyrosine Arylamidase	TYra	-ve
Growth in 6.5% NaCl	NC6.5	+ve
D-Xylose	Dxyl	-ve
L- Aspartate Arylamidase	AspA	-ve
Lactose	LAC	-ve
D- manitol	dMAN	+ve
Salicin	SAL	-ve
Arginine Dihydrolase	ADH1	-ve
Beta galactocidase	BGAR	-ve
Polymixin B resistance	POLYB	-ve
Methyl- B- D- Glucopyranoside	MBdG	-ve
D- Trehalose	dTRE	+ve
D- Galactose	dGAL	+ve
Bacitracine Resistance	BACi	+ve
Pullulan	PUL	-ve

Table 4. Effect of different concentrations mycosynthesized ZnONPs by *E. nigrum* on Vero cells.

Concentration µg/mL	Mean O.D	±SE	Viability %	Toxicity %	IC ₅₀ ± SD µg/mL
0.0	0.748	0.002309	100	0	
1000	0.043	0.002082	5.7486631	94.251337	
500	0.053	0.003606	7.0855615	92.914439	
250	0.483	0.007638	64.572193	35.427807	320.41 ± 2.17
125	0.744	0.006658	99.465241	0.5347594	
62.5	0.747667	0.001856	99.955437	0.0445633	
31.25	0.747333	0.001856	99.910873	0.0891266	

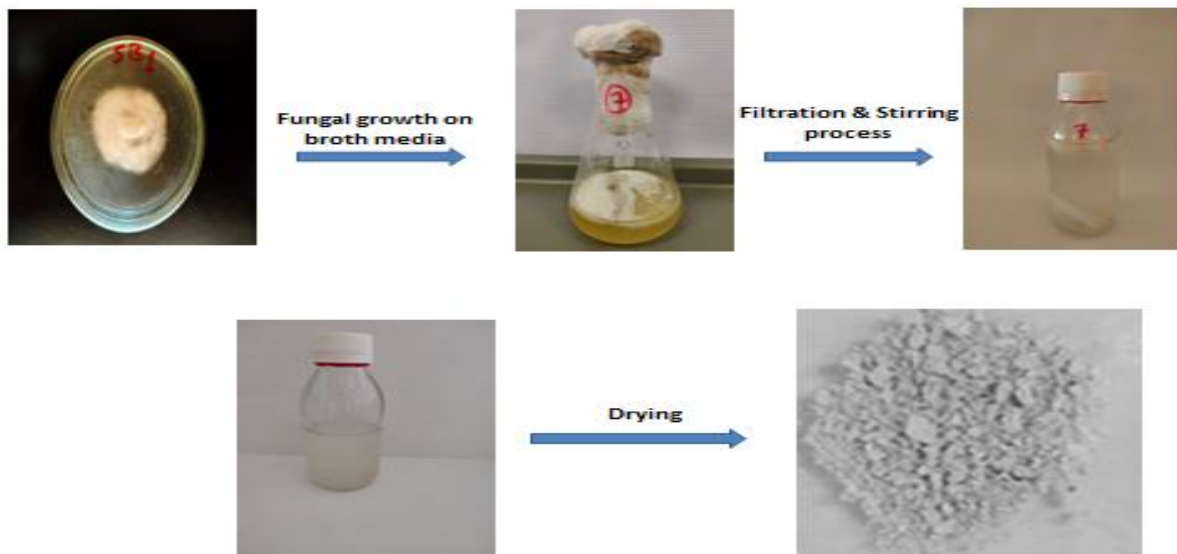
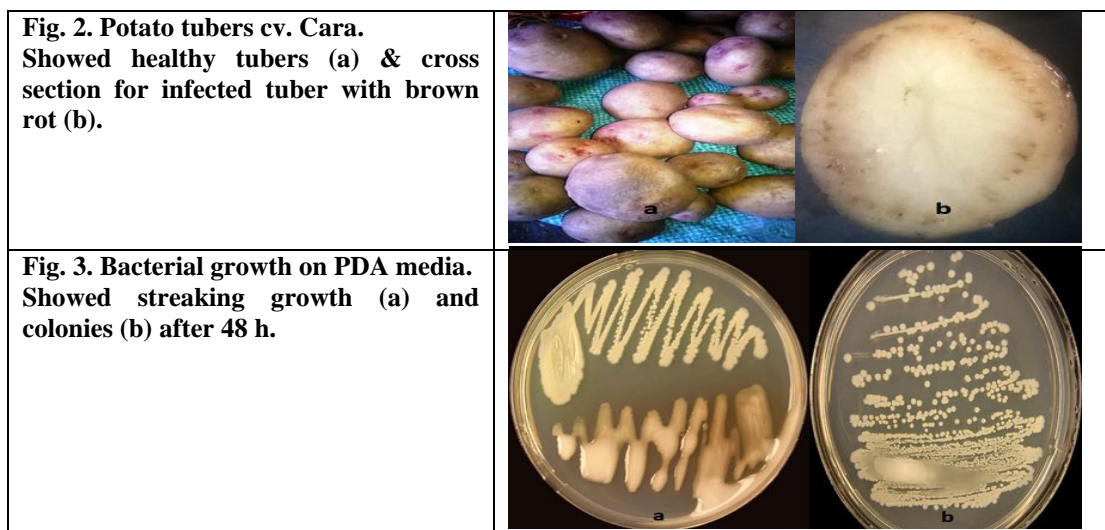


Fig. 1. Schematic presentation of mycosynthesized ZnONPs.



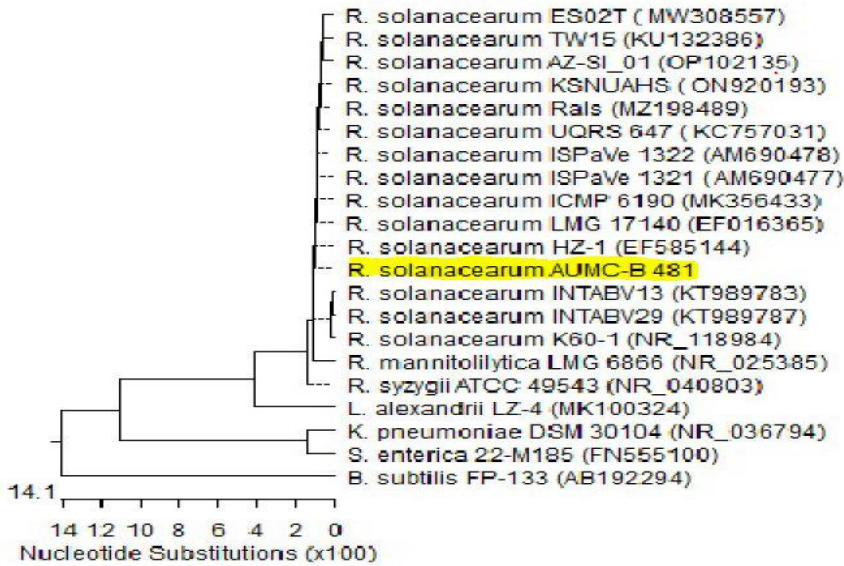
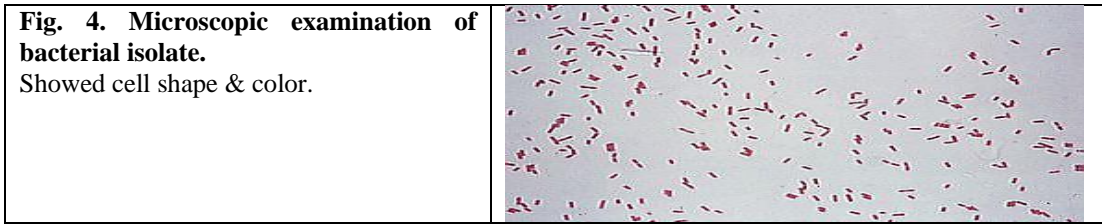
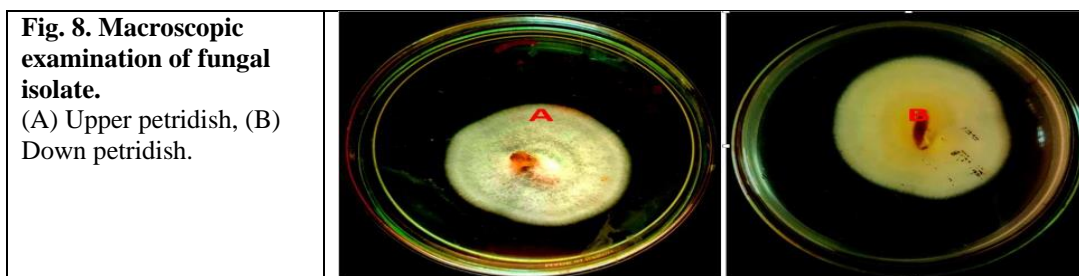
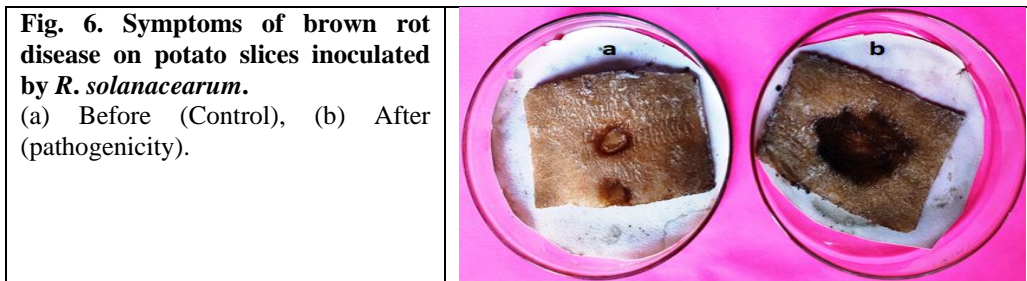


Fig. 5. Phylogenetic tree with 16S rRNA sequencing of *Ralestonia solanacearum* AUMC-B 481 (arrowed) aligned with closely similar strains accessed from the GenBank. B. = *Bacillus*, K. = *Klebsiella*, L. = *Limnobacter* and S. = *Salmonella* (outgroup strain).



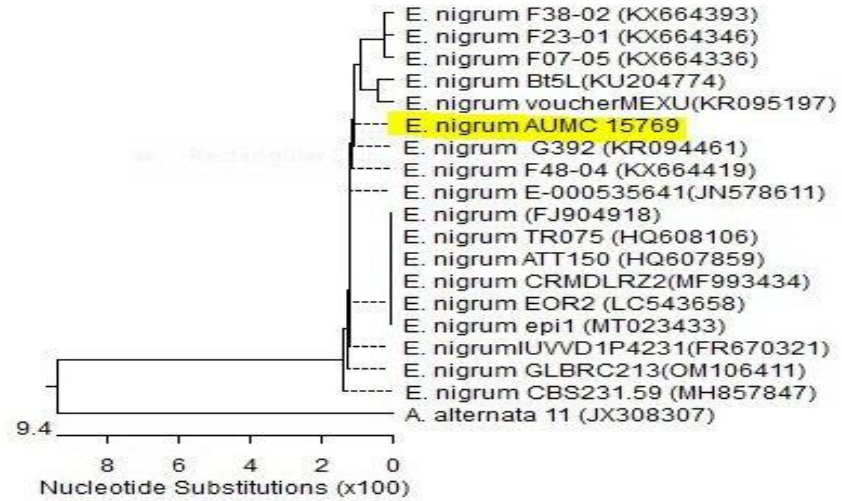


Fig. 10. Phylogenetic tree with ITS sequencing of rDNA of the fungal strain *Epicoccum nigrum* AUMC 15769 aligned with closely related sequences of fungal strains accessed from the GenBank. E. = *Epicoccum*, A. = *Alternaria* (outgroup strain).

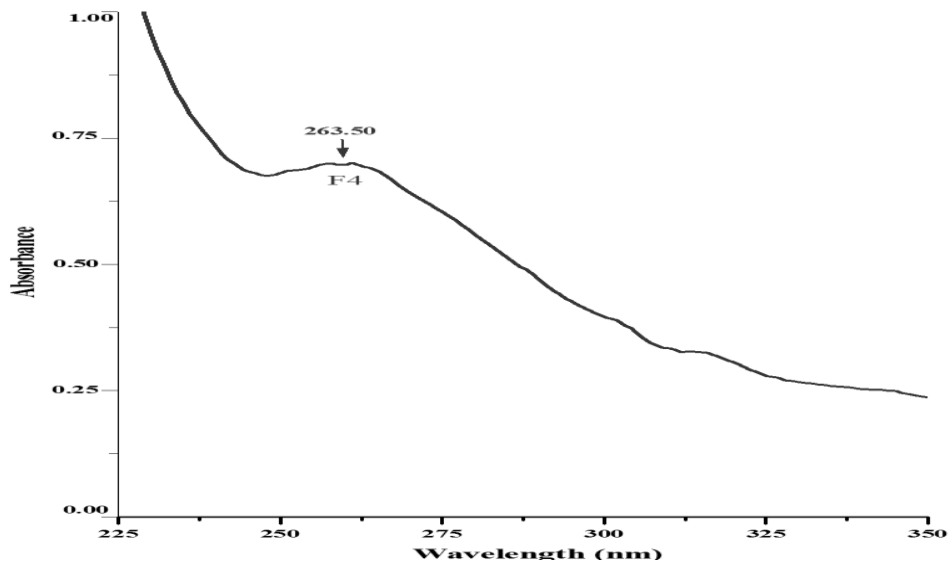


Fig. 11. UV-Vis spectra of ZnONPs synthesized by *E. nigrum*.



Fig. 12. Transmission electron micrographs of synthesized ZnONPs synthesized by *E. nigrum*.

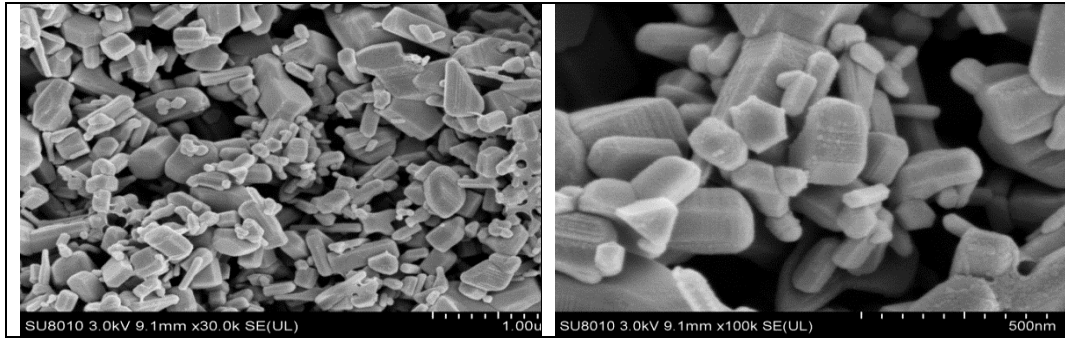


Fig. 13. SEM images of the mycosynthesized ZnONPs by *E. nigrum*.

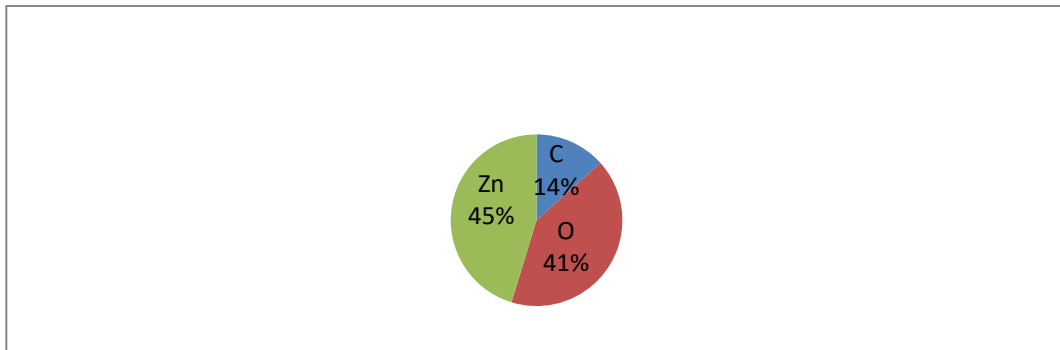


Fig. 14. Elemental composition of ZnONPs after EDX analysis.

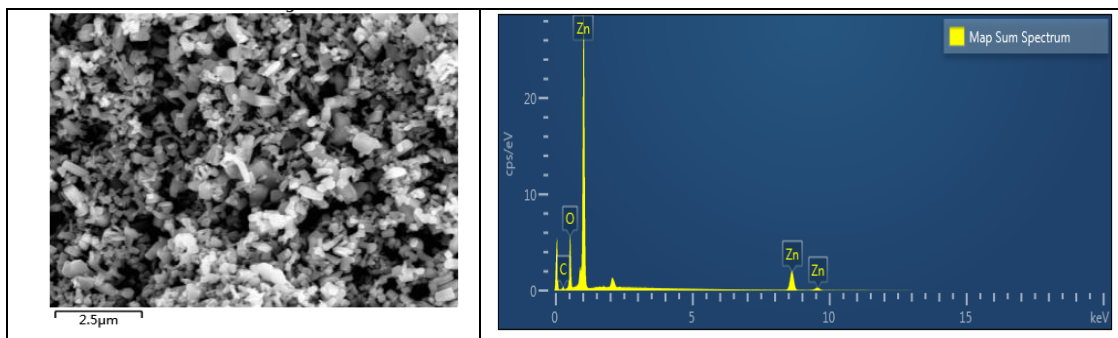


Fig. 15. EDX profile of mycosynthesized ZnONPs by *E. nigrum*.

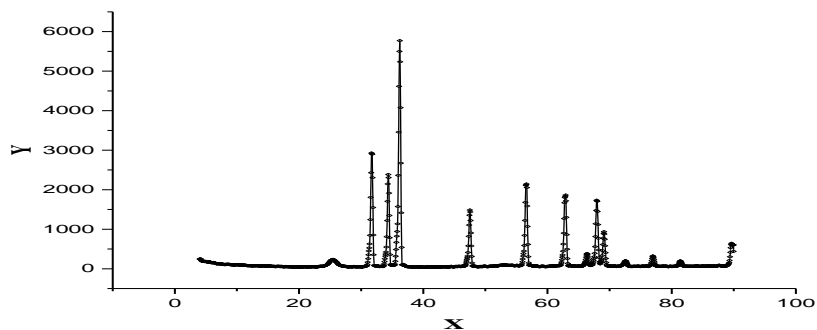


Fig. 16. XRD spectra (Y) showing the intensity a.u and (X) the 2θ in degrees of mycosynthesized ZnONPs.

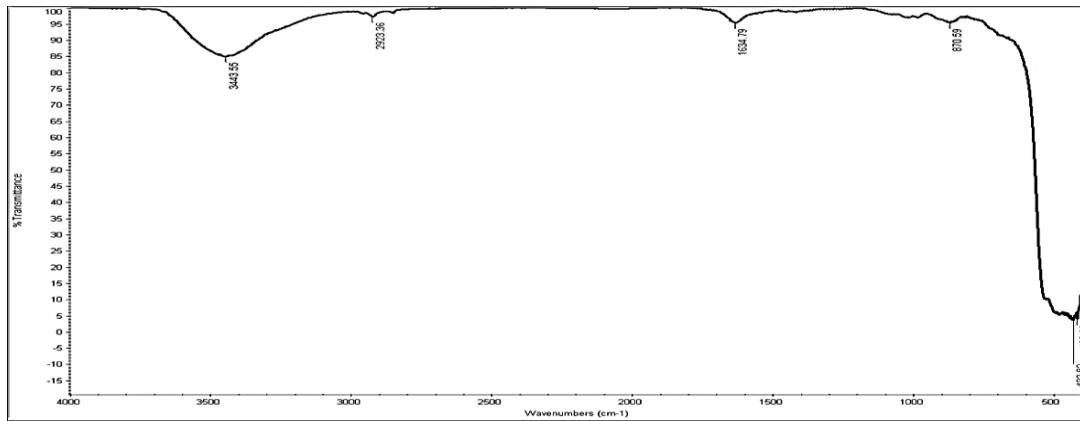


Fig. 17. FTIR spectra of ZnONPs synthesized by *E. nigrum*.

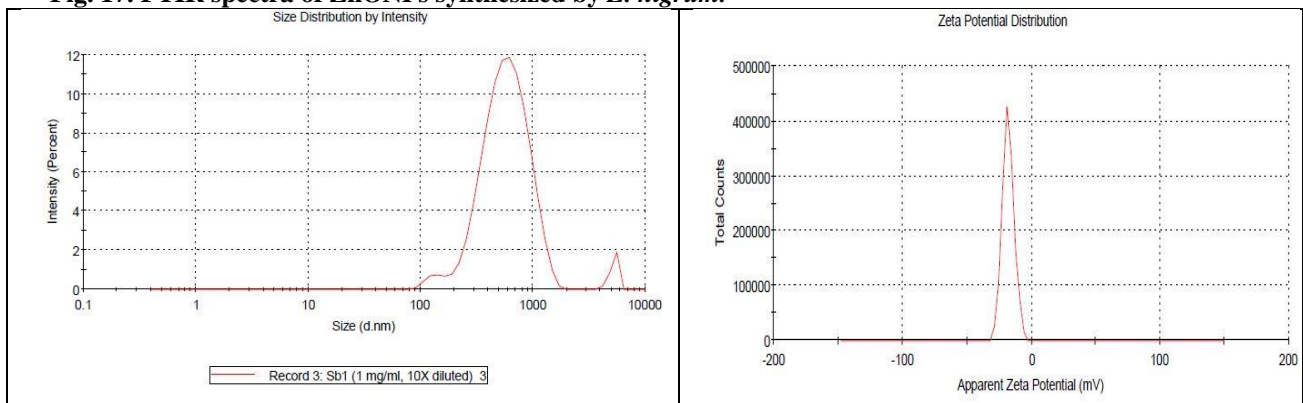


Fig. 18. Zeta potential & particle size assay of mycosynthesized ZnONPs by *E. nigrum*.

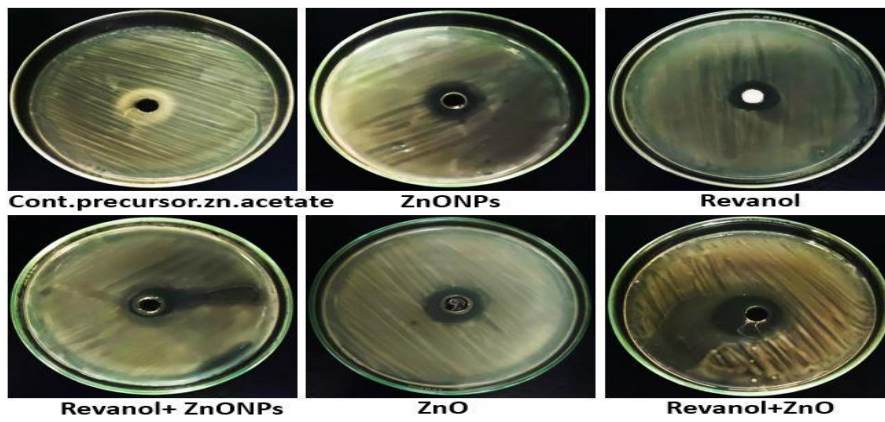


Fig. 19. Antibacterial effect of the mycosynthesized ZnONPs by *E. nigrum* with different treatments.

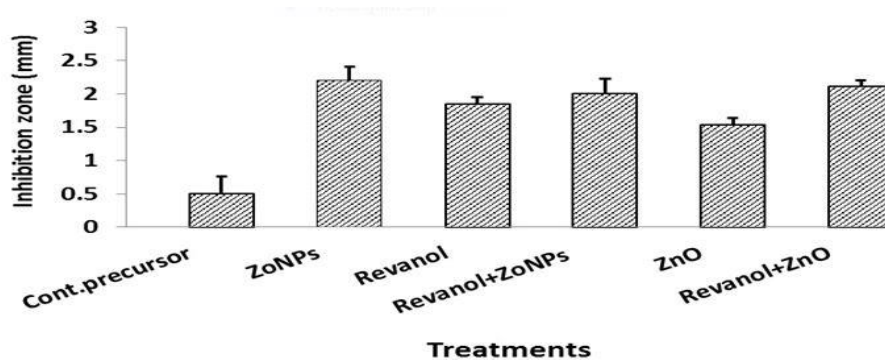


Fig. 20. Effect of mycosynthesized ZnONPs by *E. nigrum* with bacterial pathogen *in vitro*.

4. Discussion

The lost in potato crops reached about 22% which causing by microbial pathogens (Masmoudi et al., 2023), so that the progeny tolerance became weakened especially when the potato tubers offered the disease of brown rot induced by *R. solanacearum* which considered the more harmful bacterial around worldwide and losses in yield reached to 5 to 70% (Bastas, 2023). Therefore, there was a need for a safe, easy and economical method that not harmful to the health of plants, animals and therefore for humans to eradicate and treat this bacterial disease. One of the best methods, used the nanotechnology which was utilized nanomaterials or nanoparticles processes; especially used ZnONPs a played important role in destroyed the bacterial diseases in agriculture and distinguished by some features as ecofriendly substance, non-toxic and easily in the prepared as biological application (Kamal et al., 2023). Firstly, selected the most potent bacterial disease (brown rot) from visually infected cv. Cara potato tubers in the market of Elmenya governorate and isolated the pathogen organism which caused it and identified genetics as (*R. solanacearum*). Also, isolated, selected the more common isolated fungal from agricultural soil which identified genetics as (*E. nigrum*) which used in the biosynthesized of ZnONPs, The obtained data revealed that Samalout region had the highest tuber infection by bacterial diseases that results may be due to the growers repeated of potato culture at the same soil that increased the soil infestation and incidence of progeny tubers and the outcomes match up with what was reported by (Heltoft et al., 2016). The repeated potato culture in the same soil without agricultural cycle, due to increasing the soil infestation and subsequent increased the disease incidence. Disease incidence test illustrated that El-Minya growers prefers the potato culture continuously in the summer and fall seasons in the same clay soil due to the narrow and limited area this measurements lead to spread the soil infestation by bacterial disease and many authors showed that this bacteria causing wilt disease *R. solanacearum* is very difficult to control because of its ability to survive for long time in soils and ability to stay latent in the progeny of potato tubers or when cut by knives when planted as seed tubers that leading to rapid spread this result are in the same reported by (Champoiseau et al., 2009; Picard et al., 2018). Morphologically cultural identification of *R. solanacearum* demonstrated that the colonies of *R. solanacearum* on nutrient agar medium was gram

negative reaction, motile, smooth circular, raised and dirty white and small straight rod shaped according to (Anjali, 2019). MALDI process sublimates and ionizes both the sample and matrix. These created ions are separated using a TOF analyzer according to their m/z value, and the MS software then creates an MS profile by looking at these ions spectrum representations. The selected organism reached to 91% probability *R. solanacearum* with bio-number (0201704410000200) with the process of MALDI-TOF mass spectrometry (Clark, 2013). Pathogenicity test demonstrated that the tested potato tuber cv. Cara is susceptible to this bacterial pathogen either in brown rot or wilt diseases and the isolate is virulent this is the result harmony with previous study (Shmas et al., 2016). In this study, ZnONPs were biosynthesized by *E. nigrum* and evaluated for their treatment effect for the wilt or brown rot diseases and limited it. ZnONPs was prepared in vitro using fungal filtrate mixed with Zn-acetate salt as in the results with diagram (Fig. 1), this prepared solution converted to powder and occur the characterization by used some apparatus as UV-vis absorption, TEM, SEM, EDX, XRD, FTIR, Zeta potential and particle size (Kamal et al., 2016). Cytotoxicity test for ZnONPs prepared confirmation at the same ZnO nanostructures and ensured the NPs-safety, so that, the ZnONPs were enhanced the antitumor and anticancer efficacies against hepatoma, this result harmony with (Hassan et al., 2022). The cytotoxicity indicated that the effect of ZnONPs synthesized by *E. nigrum* sample against vero cells. The ZnONPs added to the vero cells with 1000 µg/mL the cell viability decreased by 5.74%. Also, the cytotoxicity increased by 94.25%. Whereas added the ZnONPs synthesized by *E. nigrum* the results with the cell viability was increased by (99.9%) & the cytotoxicity decreased by 0.08% were significant (Zhang et al., 2023). The Uv-vis absorption indicated that ZnONPs mainly show absorption peaks at wavelengths of 263.50 nm (Hefny et al., 2019), the UV visible spectra of ZnONPs showed various peaks in the range between 260 and 290 nm (Tripathy et al., 2023; Gnanamuthu & Anandan, 2023). The TEM micrographs detected that ZnONPs mycosynthesized by *E. nigrum* has a hexagonal & spherical shape and size average mean of 49.0 ± 3.0 nm (Flores et al., 2014; Manimegalai et al., 2023). The SEM graphs indicated that ZnONPs mycosynthesized by *E. nigrum* were nearby irregular in shape, this result was harmony with the previous study (Veselova et al., 2022; Manimegalai et al., 2023). The EDX profile technique confirmed that

the percentage relatively of zinc and oxygen. According to theoretical predictions based on the stoichiometric mass present and the fraction of other elements, the study ZnONPs separately conform to these assumptions are shown in (Figs. 14, 15) (El-Beley et al., 2021; Manimegalai et al., 2023). The produced nanoparticles crystallinity was measured by the XRD method and their structural characteristics were characterized. The ZnONPs exhibit unique diffraction in the spectra that are analogous to peak values and have a hexagonal crystalline structure (Misra et al., 2021; Kamal et al., 2023). The produced ZnONPs displayed a number of peaks in the FTIR analysis, suggesting the presence of the distinctive functional groups are shown in (Fig 17) (Gakis et al., 2023). The zetasizer method demonstrated that the ZnONPs average size was larger than what the TEM could measure, the heterogeneous distribution of ZnONPs in the liquid solution, which can increase particle size in the zetasizer study, may be the cause of this (Dukhin et al., 2010; Marsalek, 2014). The brown rot disease considered from the most destroyed disease for a lot of potato tubers types not only the cv. Cara but very susceptible type which the causal agent is *R. solanacearum*, related to the biological activity which ensured the antibacterial activity of ZnONPs mycosynthesized by *E. nigrum* against *R. solanacearum*, this result harmony with (He et al., 2011; Lawrence et al., 2023). So; the most prevalent bacterial disease can be prevented by using ZnONPs, which are potential biocontrol agents of potato and reduction the disease incidence (Fig 19) (Dimkpa et al., 2013; Bavarsad & Farrokhi-Nejad, 2018).

5. Conclusion

The obtained data stated from the surveying of procedures that the most common disease organisms in potato tubers were bacterial on the cv. Cara potato tubers. The bacterial disease (brown rot), El-Minya region had the highest disease incidence followed by Samalout and the lowest values was recorded in Matay, El-Edwa. The bacterial isolate identified as *R. solanacearum*, cv. Cara was susceptible. In this study, ZnONPs were successfully mycosynthesized using the most fungal isolate from native agricultural soil that molecular identified as *E. nigrum*. The nanoparticles were characterized using UV – Visible spectroscopy, TEM, SEM, EDX, XRD, FTIR, Zeta potential & particle size. Also, the cytotoxicity assay (MTT) (viability/cytotoxicity). The antibacterial ability of the ZnONPs concentration (100 µL/mL) was tested of *R. solanacearum* and it was result showed that at the potency of mycosynthesized

ZnONPs by *E. nigrum* treated the growth bacterium with zone diameter inhibition was 2.20 ± 0.20 mm which considered the maximum growth inhibition of *R. solanacearum*, but the minimum inhibition was done with control (precursor.Zn. acetate. salt) treatment by 0.50 ± 0.25 mm. Our research showed that the size of mycosynthesis ZnONPs was crucial for their effective as antibacterial potency compared to Revanol 50% as traditional product. The ZnONPs is dominant spherical & hexagonal shape small in size of 42.2 ± 3.0 nm as compared to others.

Acknowledgments

I would also want to thank Dr. Nasser Sayed Youssef, professor of vegetables at the Horticulture Research Institute and Agricultural Research Center, for his invaluable support and guidance throughout the lengthy period of my study.

Author Contributions

Conceptualization, M.S.H. and A.T.M.; methodology, formal analysis and investigation, A.M.A., A.T.M. and A.S.A.; resources and writing original draft preparation; All authors have read and agreed to the published version of the manuscript.

Funding: None.

Conflicts of Interest: The authors declare no conflict of interest

6. References

- Ababutain IM, Aldosary SK, Aljuraifani AA, Alghamdi AI, Alabdallal AH, Al-Khaldi EM, Borgio JF (2021). Identification and antibacterial characterization of endophytic fungi from *Artemisia sieberi*. *International journal of microbiology*, 2021. <https://doi.org/10.1155/2021/6651020>.
- Abbas A, Ahmad T, Hussain S, Noman M, Shahzad T, Iftikhar A, Shahid M (2022). Immobilized biogenic zinc oxide nanoparticles as photocatalysts for degradation of methylene blue dye and treatment of textile effluents. *International Journal of Environmental Science and Technology*, **19**(11), 11333-11346. <https://doi.org/10.1007/s13762-021-03872-4>.
- Abbas AM, Hammad SA, Sallam H, Mahfouz L, Ahmed MK, Abboudy SM, Mostafa M (2021). Biosynthesis of zinc oxide nanoparticles using leaf extract of *Prosopis juliflora* as potential photocatalyst for the treatment of paper mill effluent. *Applied Sciences*, **11**(23), 11394. <https://doi.org/10.3390/app112311394>.
- Abdelghany TM, Al-Rajhi AM, Yahya R, Bakri MM, Al Abboud MA, Yahya R, Salem SS (2023). Phytofabrication of zinc oxide nanoparticles with advanced characterization and its antioxidant, anticancer, and antimicrobial activity against pathogenic microorganisms. *Biomass Conversion and Biorefinery*, **13**(1), 417-430. <https://doi.org/10.1007/s13399-022-03412-1>.
- Abdelkader DH, Negm WA, Elekhrawy E, Eliwa D,

- Aldosari BN, Almurshedi, AS (2022). Zinc oxide nanoparticles as potential delivery carrier: Green synthesis by *Aspergillus niger* endophytic fungus, characterization, and *in vitro/in vivo* antibacterial activity. *Pharmaceuticals*, **15**(9), 1057. <https://doi.org/10.3390/ph15091057>.
- Abo-Elnaga HI, El-Sheikh MM, Saeed AS, Amein AM (2013). Studies on the transmission of some *Fusarium* spp. to potato progeny tubers from mother plants and its biological control. *Archives of Phytopathology and Plant Protection*, **46**(16), 1931-1948. <https://doi.org/10.1080/03235408.2013.781342>.
- Åhman J, Matuschek E, Kahlmeter G (2022). Evaluation of ten brands of pre-poured Mueller-Hinton agar plates for EUCAST disc diffusion testing. *Clinical Microbiology and Infection*, **28**(11), 1499-e1. <https://doi.org/10.1016/j.cmi.2022.05.030>.
- Ahmed W, Yang J, Tan Y, Munir S, Liu Q, Zhang J, Zhao Z (2022). *Ralstonia solanacearum*, a deadly pathogen: Revisiting the bacterial wilt biocontrol practices in tobacco and other Solanaceae. *Rhizosphere*, **21**, 100479. <https://doi.org/10.1016/j.rhisph.2022.100479>.
- Alley MC, Scudiero DA, Monks A, Hursey ML, Czerwinski MJ, Fine D, Boyd MR (1988). Feasibility of drug screening with panels of human tumor cell lines using a microculture tetrazolium assay. *Cancer research*, **48**(3), 589-601. <https://aacrjournals.org/cancerres/article/48/3/589/493419/Feasibility-of-Drug-Screening-with-Panels-of-Human>.
- Altschul SF, Gish W, Miller W, Myers EW, Lipman DJ (1990). Basic local alignment search tool. *Journal of molecular biology*, **215**(3), 403-410. [https://doi.org/10.1016/S0022-2836\(05\)80360-2](https://doi.org/10.1016/S0022-2836(05)80360-2).
- Alyokhin A, Rondon SI and Gao Y (2022). Insect pests of potato: global perspectives on biology and management. Academic Press.
- Anjali (2019). Characterisation of *Ralstonia solanacearum* (Smith) Yabuuchi et al. infecting Solanaceous vegetables in relation to physico-chemical and biological properties of soil (Doctoral dissertation, Department of Plant Pathology, College of Horticulture, Vellanikkara). <http://hdl.handle.net/123456789/9683>.
- Asaturova A, Shternshis M, Tsvetkova V, Shpatova T, Maslennikova V, Zhevnova N and Homyak A (2021). Biological control of important fungal diseases of potato and raspberry by two *Bacillus velezensis* strains. *PeerJ*, **9**, e11578. <https://doi.org/10.7717/peerj.11578>.
- Asiry KA, Shaikh BA, Abo-Elyousr KA (2021). Evaluation of Certain Essential Oil to Control of Bacterial Soft Rot of Potato Caused by *Pectobacterium carotovorum* subsp. *carotovorum*. *Journal of King Abdulaziz University: Meteorology, Environment & Arid Land Agriculture Sciences*, **30**(1). Doi: 10.4197/Met. 30-1.1.
- Aslam MN, Mukhtar T (2023). Characterization of *Ralstonia solanacearum* causing bacterial wilt from major chili growing areas of Pakistan. *Bragantia*, **82**, e20230001. <https://doi.org/10.1590/1678-4499.20230001>.
- Bastas KK (2023). Bacterial diseases of potato and their control. In *Potato Production Worldwide* (pp. 179-197). Academic Press. <https://doi.org/10.1016/B978-0-12-822925-5.00017-7>.
- Bavarsad M, Farrokhi-Nejad R (2018). Identification of *Trichoderma* Species Using Partial Sequencing of nrRNA and tef1 α Genes with Report of *Trichoderma capillare* in Iran Mycoflora. <https://doaj.org/toc/2008-4749>.
- Carmichael IS, Eugster H (2018). Thermodynamic Modeling of Geologic Materials: Minerals, Fluids, and Melts (Vol. 17). Walter de Gruyter GmbH & Co KG.
- Carter MD, Khokhani D, Allen C (2023). Cell Density-Regulated Adhesins Contribute to Early Disease Development and Adhesion in *Ralstonia solanacearum*. *Applied and environmental microbiology*, **89**(2), e01565-22. <https://doi.org/10.1128/aem.01565-22>.
- Champoiseau PG, Jones JB, Allen C (2009). *Ralstonia solanacearum* race 3 biovar 2 causes tropical losses and temperate anxieties. *Plant Health Progress*, **10**(1), 35. <https://doi.org/10.1094/PHP-2009-0313-01-RV>.
- Chokboribal J, Amornkitbamrung L, Somchit W, Suchaiya V, Khamweera P, Pankaew P (2023). Effects of ZnO/trimethylsilyl cellulose nano-composite coating on anti-UV and anti-fungal properties of papers. *Scientific Reports*, **13**(1), 20714. <https://www.nature.com/articles/s41598-023-45853-2>.
- Chugh G, Siddique KH, Solaiman ZM (2021). Nanobiotechnology for agriculture: smart technology for combating nutrient deficiencies with nanotoxicity challenges. *Sustainability*, **13**(4), 1781. <https://doi.org/10.3390/su13041781>.
- Clark A (2013). Whatever next? Predictive brains, situated agents, and the future of cognitive science. *Behavioral and brain sciences*, **36**(3), 181-204. <https://doi.org/10.1017/S0140525X12000477>.
- Dey P, Sen SK (2023). A Review On Solanaceous Plant Diseases Caused By *Ralstonia Solanacearum* Having Serious Economic Impact. *Plant Archives* (09725210), **23**(2). <https://doi.org/10.51470/Plantarchives.2023.v23.no2.072>
- Dimkpa CO, McLean JE, Britt DW, Anderson AJ (2013). Antifungal activity of ZnO nanoparticles and their interactive effect with a biocontrol bacterium on growth antagonism of the plant pathogen *Fusarium graminearum*. *Biometals*, **26**, 913-924. DOI 10.1007/s10534-013-9667-6.

- Dina AG, Aoun YA, Amr MA, Mohamed AES, Ayman ME (2022). Evaluating nanotechnology in raising the efficiency of some substances used in fertilizing wheat grown on sandy soil. *Egypt. J. Soil Sci*, **62**(2), 123 – 135. <https://doi.org/10.21608/ejss.2022.147839.151>
- Doaa TE (2024). Effect of chitosan/Jojoba oil/zno nanocomposite capsules applica. *Egypt. J. Soil Sci*. **64**(2) 673 – 698. <https://doi.org/10.21608/ejss.2024.267370.1716>.
- Dukhin AS, Goetz PJ, Fang X, Somasundaran P (2010). Monitoring nanoparticles in the presence of larger particles in liquids using acoustics and electron microscopy. *Journal of colloid and interface science*, **342**(1), 18-25. <https://doi.org/10.1016/j.jcis.2009.07.001>.
- Edslev SM, Andersen PS, Agner T, Saunte DML, Ingham AC, Johannesen TB, Clausen ML (2021). Identification of cutaneous fungi and mites in adult atopic dermatitis: analysis by targeted 18S rRNA amplicon sequencing. *BMC microbiology*, **21**, 1-8. <https://doi.org/10.1186/s12866-021-02139-9>.
- El-Belely EF, Farag MM, Said HA, Amin AS, Azab E, Gobouri AA, Fouda A (2021). Green synthesis of zinc oxide nanoparticles (ZnO-NPs) using *Arthrospira platensis* (Class: Cyanophyceae) and evaluation of their biomedical activities. *Nanomaterials*, **11**(1), 95. <https://doi.org/10.3390/nano11010095>.
- Faron ML, Buchan BW, Ledebner NA (2017). Matrix-assisted laser desorption ionization–time of flight mass spectrometry for use with positive blood cultures: methodology, performance, and optimization. *Journal of Clinical Microbiology*, **55**(12), 3328-3338. <https://doi.org/10.1128/jcm.00868-17>.
- Flores G, Carrillo J, Luna JA, Martínez R, Sierra-Fernández A, Milosevic O, Rabanal ME (2014). Synthesis, characterization and photocatalytic properties of nanostructured ZnO particles obtained by low temperature air-assisted-USP. *Advanced Powder Technology*, **25**(5), 1435-1441. <https://doi.org/10.1016/j.apt.2014.02.004>.
- Gakis GP, Aviziotis IG, Charitidis CA (2023). Metal and metal oxide nanoparticle toxicity: moving towards a more holistic structure–activity approach. *Environmental Science: Nano*, **10**(3), 761-780. <https://doi.org/10.1039/D2EN00897A>.
- Gnanamuthu F, Anandan SS (2023). Experimental Studies of Metal Oxide Suspended Nanofluids on the Enhancement of the Thermal Performance of Heat Pipes. *Transactions of FAMENA*, **47**(2), 1-12. <https://doi.org/10.21278/TOF.472046222>.
- Hashem AH, Al-Askar AA, Haponiuk J, Abd-Elsalam KA, Hasanin MS (2023). Biosynthesis, Characterization, and Antifungal Activity of Novel Trimetallic Copper Oxide–Selenium–Zinc Oxide Nanoparticles against Some Mucorales Fungi. *Microorganisms*, **11**(6), 1380. <https://doi.org/10.3390/microorganisms11061380>.
- Hassan A, Al-Salmi FA, Abuamara TM, Matar ER, Amer ME, Fayed EM, Abd El Maksoud AI (2022). Ultrastructural analysis of zinc oxide nanospheres enhances anti-tumor efficacy against Hepatoma. *Frontiers in oncology*, **12**, 933750. <https://doi.org/10.3389/fonc.2022.933750>.
- Hassan E, Shoala T, Mustafa S, Bader O, El-fiki I (2022). Salicylic Acid and Glycyrrhizic Acid Ammonium Salt in Colloidal and Nano Forms for Management of Potato Brown Rot Infection Caused by *Ralstonia solanacearum*. *New Valley Journal of Agricultural Science*, **2**(6), 296-308. <https://dx.doi.org/10.21608/nvjas.2022.161893.1086>.
- He L, Liu Y, Mustapha A, Lin M (2011). Antifungal activity of zinc oxide nanoparticles against *Botrytis cinerea* and *Penicillium expansum*. *Microbiological research*, **166**(3), 207-215. <https://doi.org/10.1016/j.micres.2010.03.003>.
- Hefny ME, El-Zamek FI, El-Fattah A, Mahgoub SAM (2019). Biosynthesis of zinc nanoparticles using culture filtrates of *Aspergillus*, *Fusarium* and *Penicillium* fungal species and their antibacterial properties against gram-positive and gram-negative bacteria. *Zagazig Journal of Agricultural Research*, **46**(6), 2009-2021. <https://dx.doi.org/10.21608/zjar.2019.51920>.
- Heltoft P, Brierley JL, Lees AK, Sullivan L, Lynott J, Hermansen A (2016). The relationship between soil inoculum and the development of *Fusarium* dry rot in potato cultivars Asterix and Saturna. *European journal of plant pathology*, **146**, 711-714. <https://dx.doi.org/10.1007/s10658-016-0946-2>.
- Innis MA, Gelfand DH (2012). *Optimization of PCRs* (pp. 3-12). Academic Press: San Diego, CA, USA.
- Kamal A, Saba M, Ullah K, Almutairi SM, AlMunqedhi BM, Ragab AM (2023). Mycosynthesis, characterization of zinc oxide nanoparticles, and its assessment in various biological activities. *Crystals*, **13**(2), 171. <https://doi.org/10.3390/cryst13020171>.
- Khairy AM, Tohamy MR, Zayed MA, Ali MA (2021). Detecting pathogenic bacterial wilt disease of potato using biochemical markers and evaluate resistant in some cultivars. *Saudi Journal of Biological Sciences*, **28**(9), 5193-5203. <https://doi.org/10.1016/j.sjbs.2021.05.045>.
- Khoshru B, Mitra D, Joshi K, Adhikari P, Rion MSI, Fadiji AE, Keswani C (2023). Decrypting the multi-functional biological activators and inducers of defense responses against biotic stresses in plants. *Heliyon*. <https://doi.org/10.1016/j.heliyon.2023.e13825>.
- Lawrence JM, Schardien K, Wigdahl B, Nonnemacher MR (2023). Roles of neuropathology-associated reactive astrocytes: A systematic review. *Acta Neuropathologica Communications*, **11**(1), 1-28. <https://doi.org/10.1186/s40478-023-01526-9>.

- Li H, Li J, Bodycomb J, Patience GS (2019). Experimental methods in chemical engineering: particle size distribution by laser diffraction—PSD. *The Canadian Journal of Chemical Engineering*, **97**(7), 1974-1981. <https://doi.org/10.1002/cjce.23480>.
- Manimegalai P, Selvam K, Loganathan S, Kirubakaran D, Shivakumar MS, Govindasamy M, Bahajjaj AAA (2023). Green synthesis of zinc oxide (ZnO) nanoparticles using aqueous leaf extract of *Hardwickia binata*: their characterizations and biological applications. *Biomass Conversion and Biorefinery*, 1-16. <https://doi.org/10.1007/s13399-023-04279-6>.
- Marquez-Villavicencio MDP, Weber B, Witherell RA, Willis DK, Charkowski AO (2011). The 3-hydroxy-2-butanone pathway is required for *Pectobacterium carotovorum* pathogenesis. *PloS one*, **6**(8), e22974. <https://doi.org/10.1371/journal.pone.0022974>.
- Marsalek R (2014). Particle size and zeta potential of ZnO. *APCBEE procedia*, **9**, 13-17. <https://doi.org/10.1016/j.apcbee.2014.01.003>.
- Masmoudi F, Alsafran M, Jabri HA, Hosseini H, Trigui M, Sayadi S, Saadaoui I (2023). Halobacteria-Based Biofertilizers: A Promising Alternative for Enhancing Soil Fertility and Crop Productivity under Biotic and Abiotic Stresses A Review. *Microorganisms*, **11**(5), 1248. <https://doi.org/10.3390/microorganisms11051248>.
- Mazurkiewicz-Pisarek A, Baran J, Ciach T (2023). Antimicrobial Peptides: Challenging Journey to the Pharmaceutical, Biomedical, and Cosmeceutical Use. *International Journal of Molecular Sciences*, **24**(10), 9031. <https://doi.org/10.3390/ijms24109031>.
- Meena M, Swapnil P, Yadav G, Sonigra P (2021). Role of fungi in bio-production of nanomaterials at megascale. In *Fungi bio-prospects in sustainable agriculture, environment and nano-technology* (pp. 453-474). Academic Press. <https://doi.org/10.1016/B978-0-12-821734-4.00006-X>.
- Misra M, Sachan A, Sachan SG (2021). Role of fungal endophytes in the green synthesis of nanoparticles and the mechanism. In *Fungi Bio-Prospects in Sustainable Agriculture, Environment and Nano-technology* (pp. 489-513). Academic Press. <https://doi.org/10.1016/B978-0-12-821734-4.00001-0>.
- Mohammad F, Pravej A, Vishnu DR, Sadia HT, Mohammad Y, Shafaque S, Muhammad FA, Shamsul H (2023). Nanoparticles: an emerging soil crops saviour under drought and heavy metal stresses. *Egypt. J. Soil Sci.* **63**(3) 355 – 366. <https://dx.doi.org/10.21608/ejss.2023.220619.1616>.
- Nasrollahzadeh M, Sajadi SM, Sajjadi M, Issaabadi Z (2019). Applications of nanotechnology in daily life. *Interface science and technology*, **28**, 113-143. <https://doi.org/10.1016/B978-0-12-813586-0.00004-3>.
- Noman M, Ahmed T, Ijaz U, Hameed A, Shahid M, Azizullah Song F (2023). Microbe-oriented nanoparticles as phytomedicines for plant health management: An emerging paradigm to achieve global food security. *Critical Reviews in Food Science and Nutrition*, **63**(25), 7489-7509. <https://doi.org/10.1080/10408398.2022.2046543>.
- Oladipo A, Enwemiwe V, Ejeromedoghene O, Adebayo A, Ogunyemi O, Fu F (2022). Production and functionalities of specialized metabolites from different organic sources. *Metabolites*, **12**(6), 534. <https://doi.org/10.3390/metabo12060534>.
- Pantidos N, Horsfall LE (2014). Biological synthesis of metallic nanoparticles by bacteria, fungi and plants. *Journal of Nanomedicine & Nanotechnology*, **5**(5), 1. <http://dx.doi.org/10.4172/2157-7439.1000233>.
- Pawaskar J, Joshi MS, Navathe S, Agale RC, Sawant Konkan Krishi Vidyapeeth B (2014). Physiological and biochemical characters of *ralstonia solanacearum*. *International Journal of Research in Agricultural Sciences*, **1**(6), 2348-3997.
- Picard C, Afonso T, Benko-Beloglavec A, Karadjova O, Matthews-Berry S, Paunovic SA, Ward M (2018). Recommended regulated non-quarantine pests (RNQP s), associated thresholds and risk management measures in the European and Mediterranean region. *EPPO Bulletin*, **48**(3), 552-568. <https://doi.org/10.1111/epp.12500>.
- Prajapati P, Gupta P, Kharwar RN, Seth CS (2023). Nitric oxide mediated regulation of ascorbate-glutathione pathway alleviates mitotic aberrations and DNA damage in *Allium cepa* L. under salinity stress. *International Journal of Phytoremediation*, **25**(4), 403-414. <https://doi.org/10.1080/15226514.2022.2086215>.
- Prusky D, Romanazzi G (2023). Induced Resistance in Fruit and Vegetables: A Host Physiological Response Limiting Postharvest Disease Development. *Annual Review of Phytopathology*, **61**. <https://doi.org/10.1146/annurev-phyto-021722-035135>.
- Rivera-Zuluaga K, Hiles R, Barua P, Caldwell D, Iyer-Pascuzzi AS (2023). Getting to the root of *Ralstonia* invasion. In *Seminars in Cell & Developmental Biology* (Vol. **148**, pp. 3-12). Academic Press. <https://doi.org/10.1016/j.semcd.2022.12.002>.
- Shaheen TI, Salem SS, Fouda A (2021). Current advances in fungal nanobiotechnology: Mycofabrication and applications. *Microbial nanobiotechnology: Principles and applications*, 113-143. https://doi.org/10.1007/978-981-33-4777-9_4.
- Shen H, Rösch P, Popp J. (2022). Fiber probe-based raman spectroscopic identification of pathogenic infection microorganisms on agar plates. *Analytical chemistry*, **94**(11), 4635-4642. <https://doi.org/10.1021/acs.analchem.1c04507>.
- Shmas AH, Ashmawy NA, El-Bebany AF, Shoeib AA (2016). Identification and Pathogenicity of

- Phytopathogenic Bacteria associated with soft rot disease on some Potato Cultivars. *Alexandria Journal of Agricultural Sciences*, **61**(6).
- Shrestha S, Wang B, Dutta P (2020). Nanoparticle processing: Understanding and controlling aggregation. *Advances in colloid and interface science*, **279**, 102162. <https://doi.org/10.1016/j.cis.2020.102162>.
- Srivastava A, Jain R, Pati PK (2022). Myconanotechnology: Green Chemistry for Sustainable Development. Bentham Science Publishers Pte. Limited.
- Tejashwini NK, Mesta RK, Hubballi M, Athani SI, Raveendra S, Biradar JI (2023). Cultural and physiological studies on Colletotrichum gloeosporioides and Fusarium oxysporum causing twister diseases in onion. <https://www.thepharmajournal.com/>.
- Tripathy P, Sethi, S, Panchal D, Prakash O, Sharma A, Mondal RB, Pal S (2023). Biogenic synthesis of nanoparticles by amalgamating microbial endophytes: potential environmental applications and future perspectives. In *Microbial Endophytes and Plant Growth* (pp. 215-231). Academic Press. <https://doi.org/10.1016/B978-0-323-90620-3.00003-9>.
- Veselova VO, Plyuta VA, Kostrov AN, Vtyurina DN, Abramov VO, Abramova AV, Ivanov VK (2022). Long-Term Antimicrobial Performance of Textiles Coated with ZnO and TiO₂ Nanoparticles in a Tropical Climate. *Journal of Functional Biomaterials*, **13**(4), 233. <https://doi.org/10.3390/jfb13040233>.
- Wang Z, Luo W, Cheng S, Zhang H, Zong J, Zhang Z (2023). *Ralstonia solanacearum*—A soil borne hidden enemy of plants: Research development in management strategies, their action mechanism and challenges. *Frontiers in Plant Science*, **14**, 1141902. <https://doi.org/10.3389/fpls.2023.1141902>.
- Yadav SA, Suvathika G, Alghuthaymi MA, Abd-Elsalam KA (2023). Fungal-derived nanoparticles for the control of plant pathogens and pests. *Fungal Cell Factories for Sustainable Nanomaterials Productions and Agricultural Applications*, 755-784. <https://doi.org/10.1016/B978-0-323-99922-9.00009-X>.
- Yadeta KA, J. Thomma BP (2013). The xylem as battleground for plant hosts and vascular wilt pathogens. *Frontiers in plant science*, **4**, 97. <https://doi.org/10.3389/fpls.2013.00097>.
- Zhang J, Islam MS, Wang J, Zhao Y, Dong W (2022). Isolation of potato endophytes and screening of *Chaetomium globosum* antimicrobial genes. *International Journal of Molecular Sciences*, **23**(9), 4611. <https://doi.org/10.3390/ijms23094611>.
- Zhang Y, Chen J, Gong H., Zhou Y, Zhang J, Li M, Cui Y (2023). Enantioselective evaluation of chiral cosmetic preservative chlorphenesin on cytotoxicity, pharmacokinetics and tissue distribution. *Microchemical Journal*, **187**, 108460. <https://doi.org/10.1016/j.microc.2023.108460>.
- Zhao L, Lu L, Wang A, Zhang H, Huang M, Wu H, Ji R (2020). Nano-biotechnology in agriculture: use of nanomaterials to promote plant growth and stress tolerance. *Journal of agricultural and food chemistry*, **68**(7), 1935-1947.